W. MOĆKO[*,**], Z.L. KOWALEWSKI[*,**]

PERFORATION TEST AS AN ACCURACY EVALUATION TOOL FOR A CONSTITUTIVE MODEL OF AUSTENITIC STEEL

WYKORZYSTANIE PRÓBY PRZEBIJANIA DO OCENY DOKŁADNOŚCI MODELU KONSTYTUTYWNEGO STALI AUSTENITYCZNEJ

In this paper, a new method for assessing the accuracy of a constitutive model is proposed. The method uses perforation test done by drop weight tower. The assessment is carried out by comparison of striker velocity curve obtained using experiment and FEM simulation.

In order to validate proposed method the various constitutive equations were applied i.e. Johnson-Cook, Zerilli-Armstrong and the extended Rusinek-Klepaczko to model mechanical behaviour of X4CrMnN16-12 austenitic steel. The steel was characterized at wide range of strain and strain rates using servo-hydraulic testing machine and split Hopkinson pressure bar.

The relative error calculated as a difference between measured and constitutive model based stress-strain curve was applied as a reference data (classic approach). Subsequently, it was compared with relative error determined on the basis of experimental and FEM calculated striker velocity (new approach). A good correlation between classic and a new method was found. Moreover, a new method of error assessment enables to validate constitutive equation in a wide range of strain rates and temperatures on the basis of a single experiment.

Keywords: plastic behaviour, fracture properties, constitutive modeling, perforation, austenitic steel

W artykule zaprezentowano nową metodę oceny dokładności modelu konstytutywnego. Oparto ją na wynikach uzyskanych w próbie przebijania z użyciem młota opadowego. Wyznaczenie błędu zostało przeprowadzone na podstawie porównania prędkości penetratora zmierzonej w trakcie eksperymentu i obliczonej na podstawie symulacji MES.

W celu walidacji metody przeanalizowano wybrane równania konstytutywne: Johnsona-Cooka, Zerilli-Armstronga oraz rozszerzony model Rusinka-Klepaczko w odniesieniu do stali austenitycznej X4CrMnN16-12. Badania właściwości mechanicznych stali zostały przeprowadzone w szerokim zakresie prędkości odkształcania z użyciem maszyny serwo-hydraulicznej oraz pręta Hopkinsona.

Błąd względny wyznaczony jako różnica zmierzonej i obliczonej na podstawie równania konstytutywnego krzywej naprężenie-odkształcenie został ustalony jako wartość błędu referencyjnego (metoda klasyczna). Następnie porównano go z błędem względnym wyznaczonym na podstawie zmierzonego i obliczonego za pomocą MES chwilowego przebiegu prędkości penetratora (nowa metoda). Stwierdzono dobrą korelację pomiędzy klasyczną a nową metodą oceny dokładności modelu. W porównaniu do klastycznej metody możliwa jest walidacja zależności konstytutywnej w szerokim zakresie prędkości odkształcania oraz temperatury w trakcie jednego testu.

1. Introduction

High-nitrogen austenitic steels have excellent physical and chemical properties, such as high strength, ductility, strong hardening effect and corrosion resistance. Therefore, these steels are often used in many applications in the automotive industry and in civil and harbour engineering. As a consequence of the wide range of potential applications, austenitic steels have become the subject of intensive scientific research related to their manufacturing process [1], their mechanical properties [2] and their micro-structural properties.

Nowadays, the rapid development of design techniques employing the Finite Element Method (FEM) can be observed.

The FEM has many advantages. This method decreases the product development time, reduces costs and allows for easier optimisation. One of the key issues in computer simulation is the accurate description of the constitutive material behaviour, which directly affects the accuracy of the calculations. As a result, numerous equations, formulas, and relations with various complication and performance levels can be found in the scientific and technical papers [3-6]. More advanced models provide a better fit for experimental data; however, these models require large quantities of data for the calibration of the coefficients, which is often measured in strictly defined experimental conditions. In cases of simple equations and a small number of parameters, the calibration process is much

* INSTITUTE OF FUNDAMENTAL TECHNOLOGICAL RESEARCH, POLISH ACADEMY OF SCIENCE, 5B PAWIŃSKIEGO STR., 02-106 WARSZAWA, POLAND

** MOTOR TRANSPORT INSTITUTE, WARSAW, POLAND

less complicated, however at the expense of fit accuracy to the experimental data.

One of the fundamental issues confronting constitutive modelling is the consistency of the model with the experimental data and its validation. Often, an accuracy of the model describing the viscoplastic properties of a material is evaluated by comparison of the measured stress/strain curves with the calculated curves for the various temperature and strain rates [7]. A drawback of this solution is that the range of the model's validation is limited to the strictly defined strain rate and temperature values that were used in the experiments. Therefore, to obtain a complete picture of the model's accuracy, many tests should be performed under various conditions.

Another method to evaluate the accuracy of a constitutive equation is to perform an experiment for a wide range of temperatures, strains and strain rates for the sample being examined. A suitable example of such method is the Taylor impact test [8], which was originally designed for determination of the material parameters at high strain rates, and is currently used for the validation of constitutive equations [9,10].

In this paper a new evaluation method for constitutive model accuracy is proposed. In this approach the measured velocity of a striker is compared with the FEM curve calculated . The examined constitutive equation is applied in the FEM code as a plasticity model. An additional advantage of the proposed solution is that the material damage initiation and evolution phenomenon can be assessed simultaneously. It has to be emphasized that this paper focuses mainly on the evaluation of the viscoplasticity model. Examples of simulations and experimental investigations of the sheet perforation process for various ambient conditions and projectile velocities can be found in other relevant studies [11, 12].

2. Experimental examinations

2.1. Determination of stress-strain curve

The X4CrMnN16-12 (VP159) austenitic high-nitrogen steel provided by the Bulgarian Academy of Sciences was used for testing in order to validate the proposed method. The chemical composition of this material is presented in Table 1. Cylindrical specimens of 6.0 mm in diameter and 3.0 mm in height were produced using the steel delivered in the form of plate subjected to electro-discharge machining (EDM).

TABLE 1

Chemical composition of the tested material

	C [%]	Si [%]	Cr [%]	Mn [%]	N_2 [%]
VP159	0.04	0.30	16.50	12.00	0.61

To determine the stress-strain curves of X4CrMnN16-12 steel, two experimental methodologies were applied [13, 14]. The first one, corresponding to a low range of strain rates, was the quasi-static compression test performed on the Instron 8801 servo-hydraulic testing machine equipped with an electromechanical extensometer. Investigations were conducted under compressive loading conditions at two strain rates: 3.2×10^{-4} s^{-1} and 9×10^{-2} s^{-1}. As the second technique the

split Hopkinson pressure bar method was applied. It enabled a material characterization under dynamic loading for strain rates of: 3.2×10^3 s^{-1}, 4.5×10^3 s^{-1}, and 6.5×10^3 s^{-1}. Due to application of both techniques a wide range of strain rates (of approximately seven orders of magnitude) was taken into account, and as a consequence, it was possible to examine the strain rate sensitivity of the constitutive equations.
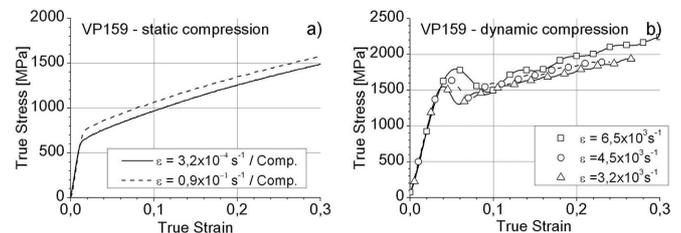

Fig. 1. Stress-strain curves of the X4CrMnN16-12 steel determined under static (a) and dynamic (b) loads

The mechanical characteristics of X4CrMnN16-12 steel obtained for quasi-static strain rates are shown in Fig. 1(a). A stress level enforcing the plastic flow increases significantly, i.e. from 800MPa to 1500 MPa within the strain range from 0.05 to 0.3 at deformation rate of 3.2×10^{-4}s^{-1}, thus illustrating a strong strain hardening effect. Among several possible reasons of such behaviour the Twining Induced Plasticity (TWIP) mechanism [15] can be indicated, however, previous analysis [14] shows that twins are already created in the material during fabrication process. Therefore, it was impossible to clearly determine whether the plastic deformation during perforation tests introduces a new twins. An increase of strain rate also causes an increase of the flow stress, indicating its high positive sensitivity to strain rate variation. The stress-strain curves determined under dynamic conditions with the use of the split Hopkinson pressure bar are presented in Fig. 1(b). Due to an extremely short duration of the deformation process, the phenomenon is of an adiabatic character. In order to bring the results into the isothermal conditions, the step loading method [16, 17] was applied.

2.2. Perforation test

The 10-mm diameter striker was manufactured using tool steel. The impact side of the striker was designed in the form of a cone with an apex angle of 30° and a rounded tip of 2 mm radius. The sample was placed between the anvil and holdfast. Both the anvil and holdfast have a circular holes of 20 mm diameter and were tied together in order to clamp the specimen. The value of a instantaneous velocity of the striker during the perforation process was measured using the Impulse system integrated with the testing stand. The striker was additionally loaded by a special additional mass to obtain 500 J impact energy under initial velocity of 12.5 m/s. As a consequence, the complete perforation of the sheet occurred.

3. Constitutive modelling

3.1. The Johnson-Cook model

The plastic flow stress can be presented as a function of strain, strain rate and temperature in a multiplicative form of

the Johnson-Cook (JC) equation [3]:

$$\sigma\left(\varepsilon, \dot{\varepsilon}, T\right) = \left(A + B\varepsilon^n\right)\left(1 + C\ln\left(\frac{\dot{\varepsilon}}{\dot{\varepsilon}_0}\right)\right)\left(1 - \left(\frac{T - T_R}{T_m - T_R}\right)^m\right),$$

(1)

where

A – yield point in the reference conditions: temperature T_R and strain rate;

B, n – strain-hardening exponents;

C – dynamic hardening exponent;

T_m – absolute temperature of the melting point;

m – coefficient of thermal softening effect.

In some cases the modified Johnson-Cook (MJC) equation can be more appropriate. In the MJC formulation the relationship between plastic flow stress and strain rate may be expressed by the power function in the following way:

$$\sigma\left(\varepsilon, \dot{\varepsilon}, T\right) = \left(A + B\varepsilon^n\right)\left(\frac{\dot{\varepsilon}}{\dot{\varepsilon}_0}\right)^C\left(1 - \left(\frac{T - T_R}{T_m - T_R}\right)^m\right)$$

(2)

This formula reflects more accurately the behaviour of a material over a wide range of strain rates. The power function better describes than the logarithmic one the effect of dynamic hardening at strain rates above 1000/s, i.e. in the range where the strain rate sensitivity rapidly increases.

The JC and MJC models are often used to describe the mechanical characteristics of materials, including various types of steel since they require only small number of parameters that must be determined. The fact that the equation is divided into three mutually independent terms describing the relationships between stress and strain and between strain rate and temperature significantly simplifies determination of the model parameters. Because the input data of the models are not conjugated, their calibration is relatively simplify. However-er, the models accuracy is low, and the range of applications is relatively narrow. The resulting values of the JC equation coefficients calculated for the steel tested are shown in Table 2, whereas those for the MJC relationship are presented in Table 3. The comparison between the experimental data and the stress/strain curves calculated on the basis of JC model is shown in Fig. 2(a), while in Fig 2(b), the data are compared for the curves calculated according to the MJC relationship.
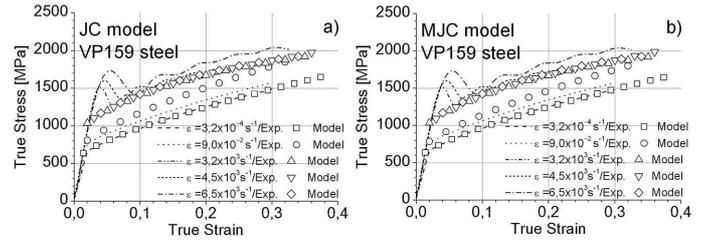

Fig. 2. Comparison between the experimental data and predicted results using the JC (a) and MJC (b) equations

3.2. The Zerilli-Armstrong model

The Zerilli and Armstrong (ZA) constitutive equation [5] is another frequently used relationship describing material behaviour under dynamic loading. For the FCC crystal lattice, the ZA model can be presented by the following equation:

$$\sigma = c_0 + B_0\varepsilon^n e^{-\left(\beta_0 - \beta_1\ln\frac{\dot{\varepsilon}}{\dot{\varepsilon}_0}\right)T},$$

(3)

where

c_0, B_0, β_0, β_1, K, n – material coefficients;

$\dot{\varepsilon}_0$ – strain rate as a reference parameter.

Similar to the JC relation, the ZA equation describes relationships between the plastic flow stress, strain, strain rate and temperature. What is new with respect to the JC equation is that the ZA equation reflects the coupled influence of temperature/strain and strain rate/temperature on the mechanical characteristics. Material constants for the ZA equation in the case of the FCC lattice steel are presented in Table 4, while the stress/strain curves elaborated according to this model are shown in Fig. 3. It can be easily noticed that a scatter between experimental and predicted results is still significant in comparison to the JC and MJC predictions.

TABLE 4

Coefficients of the ZA FCC model

Y_0 [MPa]	B_0 [MPa]	n	β_0	β_1	ε_0 [s^{-1}]	T_R [K]	T_m [K]
480	9,600	0.65	0.0052	0.00014	3×10^{-4}	296	1,800
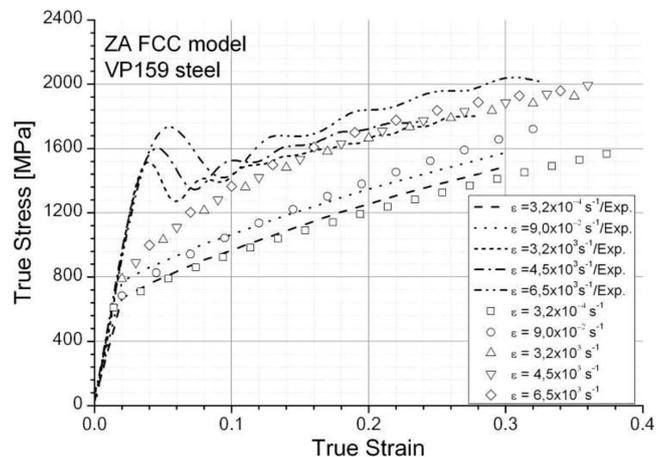
Fig. 3. Comparison of experimental stress-strain curves to those calculated according to the ZA model

TABLE 2

Coefficients of the JC model

A [MPa]	B [MPa]	n	C	m	ε_0 [s^{-1}]	T_R [K]	T_m [K]
525	2,230	0.7	0.037	0.6	3×10^{-4}	296	1,800

TABLE 3

Coefficients of the MJC model

A [MPa]	B [MPa]	n	C	m	ε_0 [s^{-1}]	T_R [K]	T_m [K]
525	2,230	0.7	0.029	0.6	3×10^{-4}	296	1,800

3.3. The Rusinek-Klepaczko model

The model proposed by Rusinek and Klepaczko (RK) [8] often presents a much more precise description of the mechanical properties variation of materials in question, particularly under dynamic loads, than the models discussed in previous sections. According to the RK model's assumptions, the equivalent stress can be decomposed into: internal stress σ_μ, effective stress σ^*, and viscous-drag stress $\bar{\sigma}_{vs}$. The relation takes into account the thermal softening of a material caused by a change in the Young's modulus variation and the dependencies between internal stress and strain, strain rate and temperature. The effective stress presented in the equation considers the coupled relationships between strain rate and temperature. The equation takes the following general form [8]:

$$\bar{\sigma}\left(\bar{\varepsilon}_p, \dot{\bar{\varepsilon}}_p, T\right) = \frac{E(T)}{E_0}\left[\sigma_\mu\left(\bar{\varepsilon}_p, \dot{\bar{\varepsilon}}_p, T\right) + \sigma * \left(\dot{\bar{\varepsilon}}_p, T\right)\right] + \bar{\sigma}_{vs}\left(\dot{\bar{\varepsilon}}_p\right), \quad (4)$$

where:

$\overline{\sigma}(\bar{\varepsilon}_p, \dot{\bar{\varepsilon}}_p, T)$– overall flow stress,
$\bar{\sigma}_\mu\left(\bar{\varepsilon}_p, \dot{\bar{\varepsilon}}_p, T\right)$ – internal stress component,
$\bar{\sigma}^*\left(\dot{\bar{\varepsilon}}_p, T\right)$ – effective stress component,
$\bar{\sigma}_{vs}\left(\dot{\bar{\varepsilon}}_p\right)$ – drag stress component,
$E(T)$– temperature dependence of the Young's modulus,
E_0 – Young's modulus at T=0K,
T – temperature,
$\dot{\bar{\varepsilon}}_p$– strain rate,
$\bar{\varepsilon}_p$– inelastic strain.

The results of the RK model calibration are presented in Table 5, whereas the stress/strain curves calculated using the model are presented in Fig. 4. As it is seen, much better fit was achieved in comparison to the models considered previously.

TABLE 5

Coefficients of the RK model

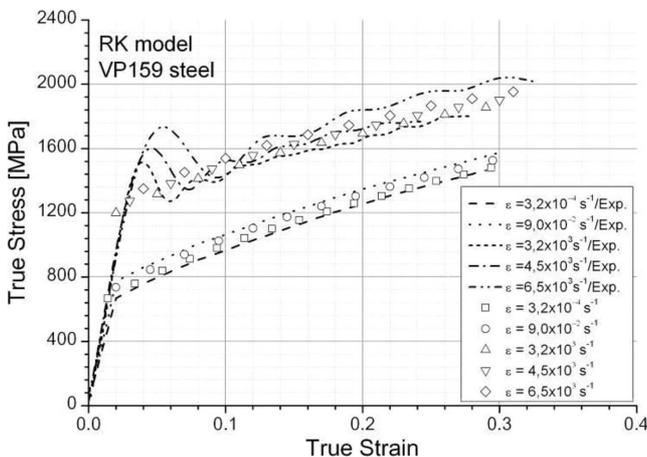| θ	B_0	υ	σ_0	D_1	m	n_0	D_2	E_ϕ [GPa]	Tm [K]	ε_{min}	ε_{max}
0,1	2560	0,05	1500	0,5	7	0,54	0,28	200	1800	10^{-5}	10^7

Fig. 4. Comparison of the experimental data and results calculated using the RK model

4. Perforation test – FEM analysis

A computer simulation of the perforation test was carried out in the ABAQUS/Explicit environment. To model the plastic behaviour of the material, the constitutive equations discussed in the third section of this paper were used. The following material constants were assumed for the steel: density 7,800 kg/m^3; Young's modulus 205 GPa; Poisson's coefficient 0.3; inelastic heat fraction 0.9; specific heat 475 J/(kgK). In order to simplify the simulation, it was assumed that the striker and the anvil are perfectly rigid bodies.

To model the material damage initiation, the Johnson-Cook criterion was used. It can be expressed by the following equation [18]:

$$\bar{\varepsilon}_D^{pl} = [d_1 + d_2 \exp\left(-d_3\eta\right)]\left[1 + d_4 \ln\left(\frac{\dot{\varepsilon}^{pl}}{\dot{\varepsilon}_0}\right)\right]\left(1 + d_5\widehat{\theta}\right) \quad (5)$$

where

$$\widehat{\theta} \equiv \begin{cases} 0 & \text{for} & \theta < \theta_{TRANS} \\ (\theta - \theta_{TRANS})/(\theta_{MELT} - \theta_{TRANS}) & \text{for} & \theta_{TRANS} \leqslant \theta \leqslant \theta_{MELT} \\ 1 & \text{for} & \theta > \theta_{MELT} \end{cases},$$

$\bar{\varepsilon}_D^{pl}$ – plastic strain at which the damage occurs; d_1-d_5 – coefficients of damage; η – stress triaxiality; θ_{MELT} – temperature of melting point; θ_{TRANS} – transition temperature; θ – current temperature; and $\dot{\varepsilon}_0$ – reference strain rate.

To determine the values of the coefficients d_1, d_2, and d_3 in equation (6), data published previously for the austenitic steel fracture at wide range of stress triaxiality were applied [19]. Due to lack of experimental data for austenitic steels in references, the results obtained by Borvik et al. [20] for Weldox 460E steel were used to determine coefficients d_4 and d_5. The calculated coefficients are presented in Table 6.

TABLE 6

Coefficients of the Johnson-Cook criterion for damage initiation of the material

d_1	d_2	d_3	d_4	d_5	θ_{TRANS}	θ_{MELT}	$\dot{\varepsilon}_0$
0.45	0.6	3	-0.0123	0	300	1,600	0.0005

Based on previous studies concerning the dynamic friction in steel [21], the friction coefficient $\mu = 0.05$ was assumed. This value has also been used by other scientists in similar experiments [22, 23]. The results of the simulation are presented in Fig. 5 in the form of the von Mises equivalent stress distribution in the sample after testing.

On the basis of FEM simulation the strain rate histogram shown in Fig. 6 was elaborated. It may be observed during perforation that strain rate decreases with the striker de-acceleration. At early stage of deformation the strain rates up to 3000 s^{-1} may be found, while values lower than 2000 s^{-1} are present near the final stage of experiment. Summarizing, it may be concluded that plastic deformation takes place under dynamic loadings at strain rates up to 3000 s^{-1}.
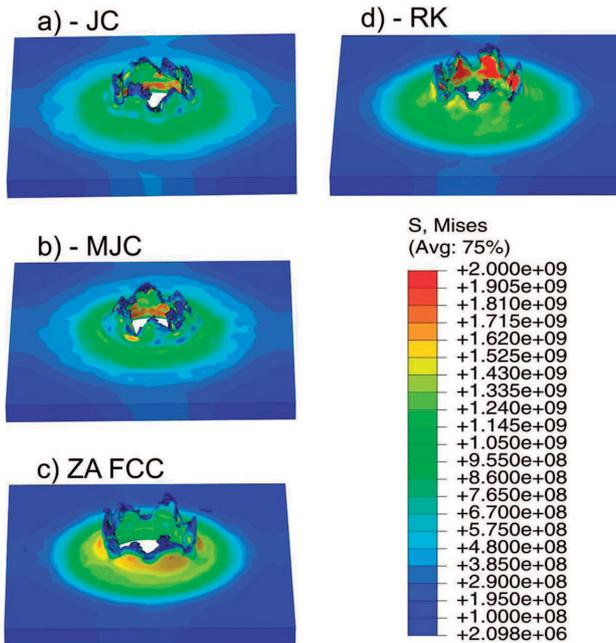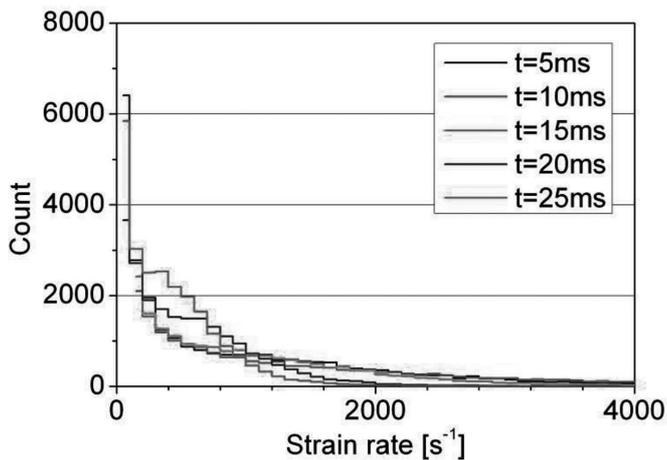
Fig. 5. Results of the FEM simulation

Fig. 6. Strain rate histogram at subsequent perforation stages

5. Validation of the models

5.1. Determination of the model error based on stress/strain curves

The accuracy of a constitutive model can be evaluated by comparison of the calculated stress/strain curves with the experimental characteristics. Therefore, the model error can be determined according to the following relationship:

$$\delta\sigma = \sum_{n=1}^{k} \int \frac{|\bar{\sigma}(\varepsilon) - \sigma(\varepsilon)|}{\sigma(\varepsilon)} d\varepsilon, \qquad (6)$$

where represents the experimental data, represents the calculated results, and n=1...k denotes the curves for various strain rates/temperatures. The result of analysis is shown in Fig. 7 and it is denoted as the "Reference". The reference data were split into two groups: obtained under quasi-static and dynamic loading conditions. The lowest values of error were found for the RK equation, while the highest ones were found for the ZA equation. The modification of the term describing the sensitivity of plastic flow stress to strain rate only slightly improved the fit of the JC model to the experimental results.
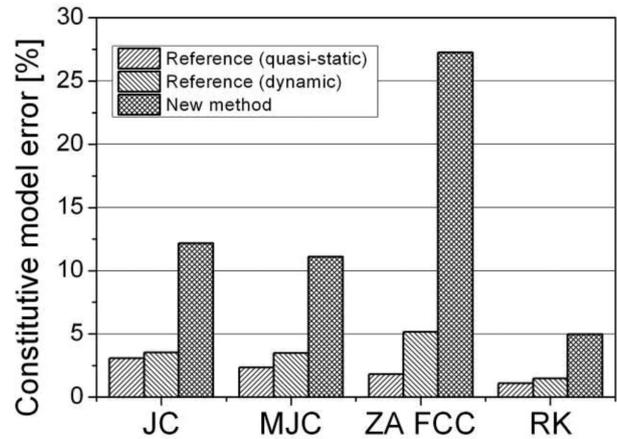

Fig. 7. Identification of the model error determined according to the proposed and reference methods

5.2. Proposed method for determination of the model error by comparing the striker velocity

An accuracy of the constitutive model may also be evaluated by comparing the measured and calculated velocity of the striker $V(t)$ during the perforation test on the basis of the following relation:

$$\delta V_{NEW} = \int \frac{\overline{V}(t) - V(t)}{|V(t)|} dt, \qquad (7)$$

where: $\overline{V}(t)$ – experimental data, and $V(t)$ – calculated results. In Fig. 8 the diagrams of calculated velocity vs. time are compared to the experimental data for the constitutive equations examined. For the ZA FCC equation, the velocity is always positive, what indicates that after the complete puncture of a sample, the striker does not stop and continues moving. In the case of experiment and for other equations taken into account, the striker stops ($V =0$) after the material perforation and subsequently reflects itself ($V<0$) in the direction opposite to the initial movement. Such an effect is connected with material elasticity, thanks to it the striker energy is stored and can be recovered due to reversible elastic strain. The model error calculated using equation (7) is presented in Fig. 7 for each constitutive relationship and indicated as the "New method". When comparing the model error determined from equations (6) and (7), a high correlation of results can be found. In both cases the highest value of error occurs for the ZA FCC equation while the lowest one occurs for the RK equations. Therefore, it can be stated that the new method enables evaluation of the model in an objective way.

The FEM analysis of the perforation test shows that the upper limit of the strain rate during the test is approximately 10^4 s^{-1} (this value is also the upper validation limit for the model analysed by this method). In the classical approach another examination method should be used in the range of strain rates considered, e.g. the miniaturised Hopkinson pressure bar or the direct impact test method [24-26].
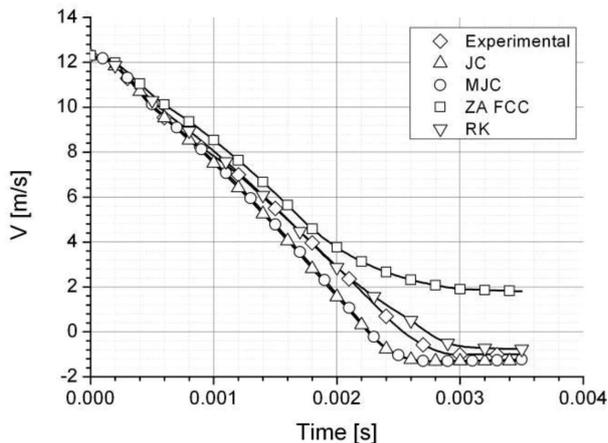
1110

Fig. 8. Velocity of the projectile during the perforation test

As a result of adiabatic heating during deformation, the sample temperature rises locally by 500°C approximately, and this level can be assumed to be the upper limit of the method validation for elevated temperatures.

6. Concluding remarks

The paper describes procedure for accuracy evaluation of a constitutive model on the basis of theoretical and experimental stress-strain characteristics and perforation test. The analysis carried out leads to the following conclusions:

- There is a strong correlation between typical method of constitutive equation error assessment and the proposed method. In both cases the ZA model gave the worst fitting results (5% and 27% calculated using old and a new method, respectively) while the RK model the best ones (2% and 5% respectively).
- By analysis of the strain rate histogram it may be found that plastic deformation process takes place under dynamic condition at rate up to $3000s^{-1}$. It may be concluded that upper limit of the new method of constitutive equation assessment is equal to 3000 s^{-1}. Therefore, the method may be applied in order to examine equation for the purposes of FEM modeling of dynamic phenomena, i.e. impact tests [27] or forging [28].
- With regard to constitutive modeling the ZA equation gave the worst results for the X4CrMnN16-12 steel tested. Presumably, such behavior may be related to a phase transformation during plastic deformation process. However, it has to be emphasized that investigation of this phenomenon was not considered in this paper.

REFERENCES

[1] H.-B. L i, Z.-H. J i a n g, M.-H. S h e n, X.-M. Y o u, J. Iron Steel Res. Int. **14**, 64-69 (2007).

[2] H.-B. L i, Z.-H. J i a n g, Z.-R. Z h a n g, B.-Y. X u, F.-B. L i u, J. Iron Steel Res. Int. **14**, 330-334 (2007).

[3] G.R. J o h n s o n, W.H. C o o k, Proceedings of Seventh International Symposium on Ballistics, The Hague, The Netherlands, pp. 541-547 (1983).

[4] A. R u s i n e k, J.R. K l e p a c z k o, Int. J. Plasticity **17**, 87-115 (2001).

[5] F.J. Z e r i l l i, R.W. A r m s t r o n g, 4 J. Appl. Phys. **61**, 1816 (1987).

[6] H. M e c k i n g, U.F. K o c k s, Acta Metall. Mater. **29**, 1865-1875 (1982).

[7] S. M a n d a l, V. R a k e s h, P.V. S i v a p r a s a d, S. V e n u - g o p a l, K.V. K a s i v i s w a n a t h a, Mat. Sci. Eng. A-Struct. **500**, 114-121 (2009).

[8] G.I. T a y l o r, J. Inst. Civ. Eng. **26**, 486-519 (1946).

[9] P.J. M a u d l i n, G.T. G r a y I I I, C.M. C a d y, G.C. K a s c h n e r, Phil. Trans. R. Soc. Lond. **A 357**, 1707-1729 (1999).

[10] S.M. W a l l e y, P.D. C h u r c h, R. T o w n s l e y, J.E. F i e l d, J. Phys. IV France. **10**, 69-74 (2000).

[11] A. R u s i n e k, J.A. R o d r ı g u e z - M a r t ı n e z, R. Z a - e r a, J.R. K l e p a c z k o, A. A r i a s, C. S a u v e l e t, Int. J. Impact Eng. **36**, 565-587 (2009).

[12] T. B ø r v i k, M.J. F o r r e s t a l, O.S. H o p p e r s t a d, T.L. W a r r e n, M. L a n g s e t h, Int. J. Impact Eng. **36**, 426-437 (2009).

[13] W. M o ć k o, Z.L. K o w a l e w s k i, Modelowanie Inżynierskie **42**, 203 (2012).

[14] W. M o ć k o, Z.L. K o w a l e w s k i, D. W o j c i e c h o w s - k i, D. R u d n i k, Biuletyn WAT **61**, 449-462 (2012).

[15] O. B o u a z i z, N. G u e l t o n, Modelling of TWIP effect on work-hardening, Mat. Sci. Eng. A-Struct. **319-321**, 246-249 (2001).

[16] S. N e m a t - N a s s e r, Y.F. L i, J.B. I s a a c s, Mech. Mater. **17**, 111-134 (1994).

[17] W. M o ć k o, Z.L. K o w a l e w s k i, Appl. Mech. Mater. **82**, 166-171 (2011).

[18] G.R. J o h n s o n, W.H. C o o k, Eng. Fract. Mech. **21**, 31-48 (1985).

[19] G. T r a t t n i g, T. A n t r e t t e r, R. P i p p a n, Eng. Fract. Mech. **75**, 223-235 (2008).

[20] T. B ø r v i k, M. L a n g s e t h, O.S. H o p p e r s t a d, K.A. M a l o, Int. J. Impact Eng. **22**, 855-886 (1999).

[21] R.S. H a r t l e y, T.J. C l o e t e, G.N. N u r i c k, Int. J. Impact Eng. **34**, 1705-1728 (2007).

[22] T. B ø r v i k, M. L a n g s e t h, O.S. H o p e r s t a d, K.A. M a l o, Int. J. Impact Eng. **27**, 37-64 (2002).

[23] J.R. K l e p a c z k o, A. R u s i n e k, J.A. R o - d r i g u e z - M a r t i n e z, R.B. P ę c h e r s k i, A. A r i a s, Mech. Mater. **41**, 599-621 (2009).

[24] J.Z. M a l i n o w s k i, J.R. K l e p a c z k o, Z.L. K o w a l e w s k i, Exp. Mech. **47**, 451 (2007).

[25] W. M o ć k o, Z.L. K o w a l e w s k i, Kovove Mater. **51**, 71 (2013).

[26] W. M o ć k o, Z.L. K o w a l e w s k i, Eng. Trans. **59**, 235-248 (2011).

[27] T. K u r s u n, Arch. Metall. Mater. **56**, 955-963.

[28] M. W o j t a s z e k, P. C h y ł a, T. Ś l e b o d a, A. Ł u k a s z e k - S o ł e k, S. B e d n a r e k, Arch. Metall. Mater. **57**, 627-635.